J. Fluid Mech. (2005), *vol.* 543, *pp.* 333–347. © 2005 Cambridge University Press
doi:10.1017/S0022112005006488 Printed in the United Kingdom

Sound produced by a vortex interacting with a cavitated wake

By M. S. HOWE

Boston University, College of Engineering, 110 Cummington Street, Boston MA 02215, USA

(Received 17 January 2005 and in revised form 9 June 2005)

A linearized analysis is made of the canonical problem of sound production during the convection of a line vortex of strength Γ in steady flow of water over a 'fence' of height h on a flat wall in the presence of a vacuous cavity in the wake of the fence. The cavity is assumed to extend sufficiently far downstream for sound waves to be regarded as launched above a non-compact, pressure-release surface. Additional vorticity is released from the tip of the fence in accordance with the Kutta condition, and is convected at the mean stream speed U along the free streamline boundary of the cavity. Sound pressures of opposite phases are generated by the incident and the shed vorticity. The predicted radiation consists of a pressure pulse of amplitude proportional to $\rho_o U\Gamma/h$ (ρ_o being the mean water density) and width approximately equal to fence height/mean flow Mach number, produced as the vortex passes the tip of the fence. The acoustic amplitude decreases rapidly at later times because of destructive interference between the sound generated by the impinging vortex and the shed vorticity.

1. Introduction

An underwater projectile can attain very high speeds if a significant part of it is enclosed within a gaseous envelope or cavity produced by a 'cavitor' situated close to the nose of the projectile (Young, Brungart & Lauchle 2004; Young *et al.* 2005). The gas 'cushions' the hydrodynamic flow and inhibits contact between the water and the surface of the projectile downstream of the cavitator. Pressure fluctuations in the separation region between the surface of the projectile and the water may be ignored, because of the great difference in mass densities between the gas and water, permitting the gas–water interface to be treated as a 'pressure-release' surface. Turbulence in the aqueous boundary layer approaching the wetted trailing edge of the cavitator from the nose generates sound and hydrodynamic pressure fluctuations as it convects across the edge, and it is of great theoretical and practical interest to determine how sound production is influenced by the pressure release interface.

Various additional sources of the sound generated by practical cavity flows of this type are readily identified. These include turbulence quadrupoles in the flow at the interface which, however, tend to be relatively unimportant because the pressure-release interface causes the quadrupole sound pressure to vary as $\rho_o v^2 M^3$, where ρ_o is the mean water density, and the Mach number $M = v/c_o \ll 1$, v being a flow velocity and c_o the mean sound speed in water (Ffowcs Williams 1974). Similarly, bubbles and water droplets in the break-up region of the cavity far downstream are respectively equivalent to monopole and dipole sources. But except at extremely high frequencies, their importance is again greatly reduced by the proximity of the

https://doi.org/10.1017/S0022112005006488 Published online by Cambridge University Press

pressure-release cavity. Observation (Young *et al.* 2005) suggests that the acoustic noise is dominated over a broad range of frequencies by the unsteady impingement of gas on the gas–water interface. Gas from a reservoir flows into the cavity as a jet, whose impingement ripples the interface and produces an unsteady surface force and an acoustic source of dipole type. The acoustic pressure generated by the dipole varies nominally as $\rho_o' v^2 M$ per unit area of the interface, where ρ_o' is the mean gas density. However, it is expected that the importance of this distributed source can be significantly reduced by careful design of the gas inlet. Edge-related sources of the type discussed in this paper would then come into prominence, since it may be anticipated that the corresponding sound pressures will scale as $\rho_o v^2 \sqrt{M}$, typical of the radiation from non-compact knife-edge flows (Ffowcs Williams & Hall 1970; Howe 1998*b*).

Young *et al.* (2004, 2005) have measured the wall pressure fluctuations just upstream of a cavity formed in the wake of a backward facing step. They report partial agreement with predictions for edge-generated fluctuations given in Young *et al.* (2005) and originally made by Howe (1998*a*) using the diffraction theory of Chase (1972, 1975) and Chandiramani (1974). The Chase–Chandiramani theory was devised for non-cavitating flow, and assumes that boundary-layer-generated edge noise corresponds to the diffracted pressure field produced when a prescribed 'frozen' pattern of hydrodynamic wall pressure fluctuations convects over the edge. Predictions of the acoustic radiation by this means agree well with edge-noise measurements at low Mach numbers, provided a suitable empirical model is available for the spectrum of the incident frozen pressure field (Blake 1986). The theory implicitly imposes the Kutta condition that velocity fluctuations must remain finite at the upstream edge of the cavity.

In the present paper a theoretical investigation is made of a canonical edge–cavity interaction problem, involving nominally steady two-dimensional inviscid flow of water at speed U along a flat wall towards a 'fence' of finite height h to the rear of which is formed a cavity of the Kirchhoff–Rayleigh type (Birkhoff & Zarontonello 1957; Rayleigh 1876), as illustrated in figure 1(*a*). A line vortex of strength Γ is embedded in the flow and aligned parallel to the fence. The vortex is swept over the fence thereby perturbing the free streamline boundary of the cavity and causing sound waves to radiate away into the water. The vortex may be regarded as a single element in the turbulent flow past the fence. Although the longitudinal coherence of such a vortex does not permit it to be fully representative of a real three-dimensional eddy, it is known (e.g. see Crighton 1975; Howe 1998*b*) how to generalize hydroacoustic scaling laws from two to three spatial dimensions, so that a full understanding of this two-dimensional problem is not without practical significance.

The problem is geometrically nonlinear, but can be solved in a first approximation by assuming the vortex to be sufficiently weak ($\Gamma \ll hU$) that it is convected passively past the fence at the local undisturbed mean velocity. This condition is effectively equivalent to the usual edge-noise approximation, that boundary layer turbulence may be regarded as 'frozen' during convection by the mean flow across the edge interaction region (Blake 1986; Chase 1972, 1975). It is known from experiment that identifiable turbulence structures convect typically at about 70% of the mean stream velocity, which is very much larger than likely nonlinear convection velocities produced by images and neighbouring eddies. Fluctuations everywhere within the fluid, including at the free streamline, will therefore be taken to be governed by the equations of motion linearized about the nonlinear mean flow. In the absence of geometrical nonlinearity, when the flow is of the type indicated in figure 1(*b*), where

https://doi.org/10.1017/S0022112005006488 Published online by Cambridge University Press

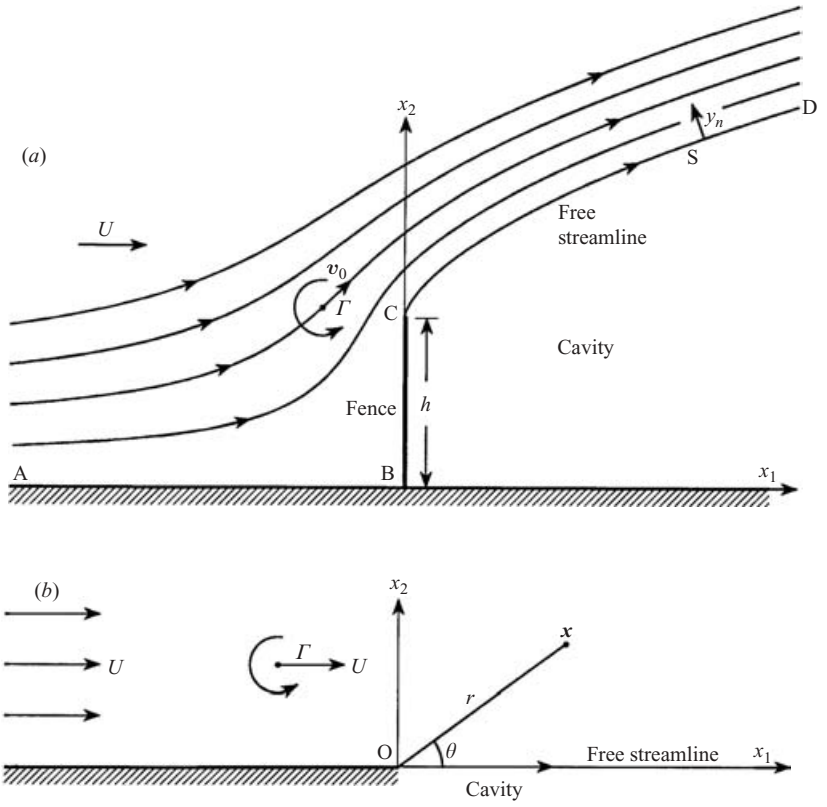


FIGURE 1. (*a*) Passive convection of a line vortex Γ in Kirchhoff–Rayleigh free streamline flow of water past a fence of height h. (*b*) Convection of a vortex in uniform flow past a half-plane with a free streamline wake.

the free streamline of the cavity can be regarded as the continuation of the wall, linear theory predicts that no sound is produced during the passage of the vortex – in precise agreement with the corresponding prediction for trailing-edge noise in the absence of cavitation. This occurs because linear theory in these circumstances requires the vortex Γ and the shed vorticity on the free streamline to convect parallel to the wall at the same speed (Howe 1976, 1998*b*). Any radiation from the edge is then relatively weak and second order in the perturbation amplitude ($\sim O(\Gamma^2)$). Such cancellation would not be expected for flow past the fence, however, because the acceleration of the mean flow is different on neighbouring streamlines in the vicinity of the edge of the fence.

The aeroacoustic problem is formulated in § 2. The hydrodynamic near-field properties of the unsteady flow are determined according to linear theory with a Kutta condition applied in § 3 and the sound radiated from the fence is then calculated (§ 4).

2. Formulation of the problem

Consider the nominally steady two-dimensional irrotational flow of water at speed U parallel to the rigid wall $x_2 = 0$ of figure 1(*a*), where the origin of coordinates $\boldsymbol{x} = (x_1, x_2)$ is taken at the foot B of the fence BC. A free streamline separates

https://doi.org/10.1017/S0022112005006488 Published online by Cambridge University Press

smoothly from the tip C of the fence forming the boundary CD of a cavity wherein the pressure p vanishes, such that the mean flow speed on the free streamline is U. The motion is assumed to be linearly disturbed from the steady state by a line vortex of strength $\Gamma \ll hU$ situated at $\boldsymbol{x} = \boldsymbol{x}_o(t)$ at time t. In this approximation the influence on the vortex of the image system formed in the rigid boundaries and the free streamline is negligible, so that the vortex is swept over the fence along a streamline of the undisturbed flow at the local mean flow velocity $\boldsymbol{v}_o(\boldsymbol{x})$, say.

The sound generated as the vortex passes the fence will be calculated by application of Lighthill's acoustic analogy (Howe 1998*b*). In all practical flows of the present type the mean flow Mach number is infinitesimal, so that convection of sound by the mean flow can be neglected. The 'vortex sound' formulation of Lighthill's equation then reduces to the form (Howe 1998*b*)

$$\left(\frac{1}{c_o^2}\frac{\partial^2}{\partial t^2} - \nabla^2\right) B = \operatorname{div}(\boldsymbol{\omega} \wedge \boldsymbol{v}), \tag{2.1}$$

where $B = p/\rho_o + \frac{1}{2}v^2$ is the total enthalpy, ρ_o, c_o are respectively the mean density and sound speed in the water, $\boldsymbol{v} \equiv \boldsymbol{v}(\boldsymbol{x}, t)$ the flow velocity, and $\boldsymbol{\omega} = \operatorname{curl} \boldsymbol{v}$ is the vorticity. Recall that $B \equiv -\partial\varphi/\partial t$ in those regions where the motion is irrotational and described by a velocity potential φ. Therefore it may be assumed that $B \equiv 0$ in the steady state (in the absence of the vortex). Viscous dissipation is ignored within the body of the fluid, but its role in diffusing vorticity from the fence will be implicitly included in the analysis of the motion by application of the Kutta condition at the tip of the fence (Crighton 1985).

The right-hand side of equation (2.1) is assumed to be known and the solution $B(\boldsymbol{x}, t)$ determines the sound radiated during the interaction of the vortex with the fence. The solution must satisfy the condition of vanishing normal component of velocity on the wetted section ABC of the wall and fence, and (in the linearized approximation) vanishing pressure on the undisturbed mean free streamline S. A formal representation of $B(\boldsymbol{x}, t)$ can be written down by introducing a Green's function $G(\boldsymbol{x}, \boldsymbol{y}, t-\tau)$, which is a solution of (2.1) with outgoing wave behaviour when the right-hand side is replaced by the impulsive point source $\delta(\boldsymbol{x} - \boldsymbol{y})\delta(t-\tau)$. A unique specification of G is obtained by requiring it to have vanishing normal derivative on the rigid boundary ABC of the flow and to vanish on the free boundary S. Then (see Howe 1998*b* for detailed manipulations)

$$B(\boldsymbol{x}, t) = -\int (\boldsymbol{\omega} \wedge \boldsymbol{v})(\boldsymbol{y}, \tau) \cdot \frac{\partial G}{\partial \boldsymbol{y}}(\boldsymbol{x}, \boldsymbol{y}, t-\tau)\, \mathrm{d}^2\boldsymbol{y}\, \mathrm{d}\tau + \int_{\mathrm{S}} B(s, \tau)\frac{\partial G}{\partial y_n}(\boldsymbol{x}, \boldsymbol{y}, t-\tau)\, \mathrm{d}s\, \mathrm{d}\tau. \tag{2.2}$$

In these integrals the temporal integrations with respect to τ extend over all possible values of the retarded time $(-\infty, \infty)$, and $s \equiv s(\boldsymbol{y})$ is distance measured along the mean free streamline from the tip of the fence. The first integral is over the fluid region where $\boldsymbol{\omega} \neq \boldsymbol{0}$, and is therefore confined to the infinitesimal cross-section of the vortex Γ. The second is taken along the undisturbed free streamline S, and y_n is distance measured normal to the streamline and to the left of the direction of the mean flow (from S into the fluid).

Now $\boldsymbol{\omega} = \Gamma\boldsymbol{k}\delta(\boldsymbol{y} - \boldsymbol{x}_o(\tau))$ and $\boldsymbol{v}(\boldsymbol{x}_o(\tau), \tau) \equiv \boldsymbol{v}_o(\boldsymbol{x}_o(\tau))$ in the linearized approximation, where $\boldsymbol{k}$ is a unit vector out of the plane of the paper in figure 1(*a*).

https://doi.org/10.1017/S0022112005006488 Published online by Cambridge University Press

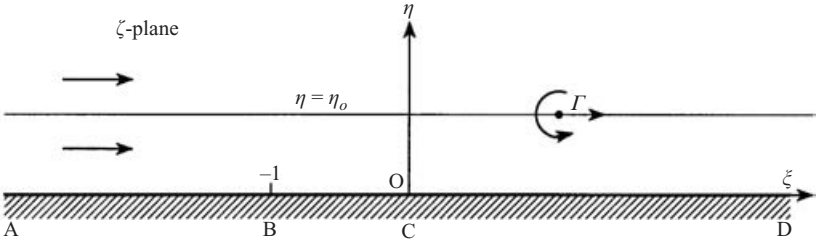


FIGURE 2. Image of the hydrodynamic flow in the upper ζ-plane.

Therefore (2.2) becomes

$$B(\boldsymbol{x}, t) = -\Gamma \int v_o(\boldsymbol{x}_o(\tau)) \frac{\partial G}{\partial y_n}(\boldsymbol{x}, \boldsymbol{x}_o(\tau), t-\tau)\, \mathrm{d}\tau + \int_{\mathrm{S}} B(s, \tau) \frac{\partial G}{\partial y_n}(\boldsymbol{x}, \boldsymbol{y}, t-\tau)\, \mathrm{d}s\, \mathrm{d}\tau. \tag{2.3}$$

The first integral can be performed once the functional form of Green's function is specified. To evaluate the integral over the free streamline it is first necessary to determine $B(s, t)$ on S.

3. Hydrodynamic interaction of the vortex and fence

At very low mean flow Mach number $M = U/c_o$ the wavelength of sound generated by the interaction $\sim h/M$ ($\gg h$) is very much larger than the interaction region and the details of the local motion in the neighbourhood of the fence can be calculated by assuming the flow to be incompressible. When the motion is only linearly disturbed from the steady state by the vortex Γ the calculation is readily performed in terms of the mapping of the undisturbed region of flow in the z-plane ($z = x_1 + \mathrm{i}x_2$) onto the upper half of the ζ-plane (figure 2).

3.1. *The mean flow*

Let the boundary ABCD of the undisturbed mean flow be mapped onto the real ζ-axis with the correspondences indicated in figure 2, with the tip C ($z = \mathrm{i}h$) and the foot B ($z = 0$) of the fence mapping respectively into the $\zeta = 0$ and $\zeta = -1$. Then the complex potential w_o of the mean flow and the transformation are given by (Lamb 1932; Batchelor 1967; Birkhoff & Zarantonello 1957; Gurevich 1965)

$$\left.\begin{aligned} w_o &= \frac{2hU\zeta}{\pi + 4}, && (3.1a)\\ z &= \frac{\mathrm{i}\pi h}{\pi + 4} + \frac{2h}{\pi + 4}[\sqrt{\zeta}\sqrt{\zeta + 1} - \ln(\sqrt{\zeta} + \sqrt{\zeta + 1}) + 2\mathrm{i}\sqrt{\zeta + 1}], && (3.1b) \end{aligned}\right\} \eta \geqslant 0,$$

where $\zeta = \xi + \mathrm{i}\eta$ (ξ, η being the real and imaginary parts of ζ) and the principal values of the square roots and the logarithm are to be taken.

The streamlines of the mean flow are the family of curves $\eta(x_1, x_2) =$ constant; the mean flow velocity is given by

$$\boldsymbol{v}_o = \frac{2hU}{\pi + 4} \nabla\xi(x_1, x_2). \tag{3.2}$$

https://doi.org/10.1017/S0022112005006488 Published online by Cambridge University Press

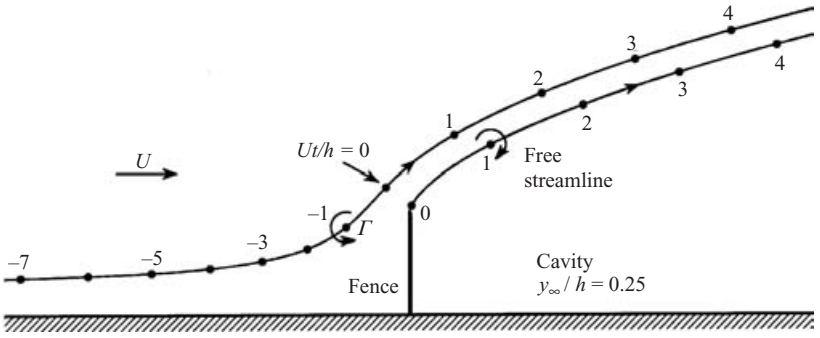


FIGURE 3. The upper curve represents the numerical solution of (3.3) defining the motion of the vortex Γ past the fence when $y_\infty = 0.25h$. The vortex passes through the points • at the indicated non-dimensional times Ut/h, measured from the instant at which the vortex is closest to the tip of the fence. The points on the free streamline correspond to successive positions of the peak in the value of the circulation density $\gamma(t - s/U)$ of figure 5.

3.2. *Motion of the vortex*

In the linearized approximation the complex position $z_o = x_{1o} + \mathrm{i}x_{2o}$ of the vortex at time t is determined by the equation of motion $\mathrm{d}z_o^*/\mathrm{d}t = (\mathrm{d}w_o/\mathrm{d}z)_{z=z_o}$. This must be solved numerically, and this is conveniently done by considering the motion of the image vortex in the ζ-plane at $\zeta = \zeta_o(t) \equiv \xi_o(t) + \mathrm{i}\eta_o$, which travels along a straight line $\eta_o =$ constant. If $x_{2o} = y_\infty$ is the asymptotic distance of the vortex from the wall at positions far upstream of the fence, equation (3.1) then implies that

$$\frac{\mathrm{d}\xi_o}{\mathrm{d}\hat{t}} = \frac{h}{U}\frac{\mathrm{d}w_o}{\mathrm{d}\zeta}\left|\left(\frac{\mathrm{d}\zeta}{\mathrm{d}z}\right)_{z=z_o}\right|^2 \equiv \frac{(\pi+4)}{2}\left|\frac{\sqrt{\zeta_o+1}}{\sqrt{\zeta_o}+\mathrm{i}}\right|^2, \quad \hat{t} = \frac{Ut}{h}, \quad \eta_o = \frac{y_\infty(\pi+4)}{2h}. \tag{3.3}$$

This determines $\zeta_o \equiv \zeta_o(\hat{t})$ as a function of the non-dimensional time Ut/h. The position $z_o(\hat{t})$ in the physical plane is found by substitution of the solution into equation (3.1*b*).

The upper curve in figure 3 depicts the path of the vortex when $y_\infty = 0.25h$. The points labelled on the curve give the position of Γ at different values of Ut/h, measured from the instant at which the vortex is at its shortest distance from the tip of the fence. The variable spacing between these points indicates how the vortex convection speed v_o decreases as the vortex approaches the fence and then accelerates to $v_o = U$ as it passes the tip.

3.3. *The hydrodynamic approximation*

In the absence of the vortex it can be assumed that B vanishes everywhere. As the vortex passes the fence $B(\boldsymbol{x}, t)$ is linearly perturbed about this value. The hydrodynamic components of the fluctuations dominate the motion in the near field of the fence, and are determined by Lighthill's equation (2.1) with the term in c_o on the left-hand side discarded. The solution $B(\boldsymbol{x}, t)$ of this modified equation is required in order to evaluate the second integral in (2.3).

The solution can be effected by transforming to the ζ-plane. First note that

$$\delta(\boldsymbol{x} - \boldsymbol{x}_o) = \left|\frac{\mathrm{d}\zeta}{\mathrm{d}z}\right|^2 \delta(\xi - \xi_o)\delta(\eta - \eta_o) \tag{3.4}$$

https://doi.org/10.1017/S0022112005006488 Published online by Cambridge University Press

and that the Cauchy–Riemann equations imply

$$\boldsymbol{\omega}\wedge\boldsymbol{v} \;\equiv\; \frac{2hU\Gamma}{\pi+4}(\boldsymbol{k}\wedge\nabla\xi)\,\delta(\boldsymbol{x}-\boldsymbol{x}_o) \;=\; \frac{2hU\Gamma}{\pi+4}\left|\frac{\mathrm{d}\zeta}{\mathrm{d}z}\right|^2\nabla\eta\,\delta(\xi-\xi_o)\delta(\eta-\eta_o). \tag{3.5}$$

Then the hydrodynamic form of (2.1) becomes in the ζ-plane

$$\left(\frac{\partial^2}{\partial\xi^2}+\frac{\partial^2}{\partial\eta^2}\right)B = -\frac{2hU\Gamma}{\pi+4}\left|\left(\frac{\mathrm{d}\zeta}{\mathrm{d}z}\right)_o\right|^2\delta(\xi-\xi_o)\delta'(\eta-\eta_o), \tag{3.6}$$

where $(\mathrm{d}\zeta/\mathrm{d}z)_o$ is evaluated at $z=z_o$ and the prime denotes differentiation with respect to the argument. The solution is required in $\eta>0$.

In irrotational regions $B\equiv-\partial\varphi/\partial t$, so that B must satisfy $\partial B/\partial\eta=0$ on the section $-\infty<\xi<0$ of the real axis. To obtain the appropriate condition on the positive real axis, observe that Bernoulli's equation implies that, except at the point occupied by the vortex,

$$\frac{\partial\varphi}{\partial t}+\frac{\delta p}{\rho_o}+\boldsymbol{v}_o\cdot\nabla\varphi=0,$$

where δp and φ denote respectively the perturbation pressure and velocity potential induced by the passage of the vortex. This equation remains valid on a fixed control surface close to the perturbed free streamline, and δp and φ must differ from their respective free streamline values by terms of second order. Hence, because $\delta p=0$ on the perturbed free streamline, the potential φ satisfies to first order $\partial\varphi/\partial t+U\partial\varphi/\partial s=0$ on S (where $v_o\approx U$). Thus, because $\mathrm{d}s=2h\,\mathrm{d}\xi/(\pi+4)$ on S, the corresponding condition on the image $\xi>0,\ \eta=0$ of the free streamline becomes $\partial B/\partial t+\{(\pi+4)U/2h\}\partial B/\partial\xi=0$.

Equation (3.6) may now be solved by setting

$$B=B_I+B_s \tag{3.7}$$

where $B_I(\xi,\eta,t)$ is the particular integral equal to the 'free space' solution when the boundary at $\eta=0$ is ignored. This decays with distance from the source and can be expressed as the double Fourier integral

$$B_I=\frac{\mathrm{sgn}(\eta-\eta_o)}{4\pi}\int_{-\infty}^{\infty}\mathscr{F}(k,\omega)\mathrm{e}^{\mathrm{i}(k\xi-\omega t)-|k||\eta-\eta_o|}\,\mathrm{d}k\,\mathrm{d}\omega \tag{3.8}$$

where $\mathscr{F}(k,\omega)$ is the Fourier transform of the source term on the right of (3.6) with respect to its dependances on ξ and t, given by

$$\mathscr{F}(k,\omega)=\frac{-\Gamma Uh}{\pi(\pi+4)}\int_{-\infty}^{\infty}\left|\frac{\mathrm{d}\zeta_o}{\mathrm{d}z}(\tau)\right|^2\mathrm{e}^{-\mathrm{i}(k\xi_o(\tau)-\omega\tau)}\,\mathrm{d}\tau, \tag{3.9}$$

in which $\mathrm{d}\zeta_o/\mathrm{d}z$ is known as a function of time from the numerical solution of (3.3).

The component $B_s(\xi,\eta,t)$ is the bounded solution of Laplace's equation $(\partial^2/\partial\xi^2+\partial^2/\partial\eta^2)B_s=0$ in $\eta>0$ satisfying

$$\left.\begin{aligned}\frac{\partial B}{\partial\eta}&=0, \quad \xi<0,\\ \frac{\partial B}{\partial t}+\frac{(\pi+4)U}{2h}\frac{\partial B}{\partial\xi}&=0, \quad \xi>0,\end{aligned}\right\}\ \eta=0. \tag{3.10a,b}$$

In addition the Kutta condition is imposed by requiring $\partial B_s/\partial\eta$ to remain finite at the image $\zeta=0$ of the tip of the fence. This is a standard Wiener–Hopf problem (Noble

https://doi.org/10.1017/S0022112005006488 Published online by Cambridge University Press

1958) that is readily solved by first determining B_s for each Fourier component of B_I proportional to $\mathrm{e}^{\mathrm{i}(k\xi-\omega t)-|k||\eta-\eta_o|}$.

To solve the aeroacoustic problem using (2.3) it is necessary to know the behaviour of B only on the free streamline ($\eta = 0,\ \xi > 0$). Condition (3.10*b*) implies that fluctuations in B propagate without change as wave-like disturbances from the image $\zeta = 0$ of the fence tip along the free streamline $\eta = 0$ at constant speed $\mathrm{d}\xi/\mathrm{d}t = (\pi+4)U/2h$ (at speed U in the physical plane), and that for each Fourier component of the incident disturbance we can write

$$B = \alpha(k,\omega,\eta_o)\mathrm{e}^{\mathrm{i}(\nu\xi-\omega t)}, \quad \nu = \frac{2\omega h}{(\pi+4)U}, \quad \text{for } \xi > 0,\ \eta = 0.$$

The wave amplitude $\alpha(k,\omega,\eta_o)$ is fixed by the Kutta condition. The procedure for its application is identical with that used in analogous treatments of small-amplitude vortex shedding from flat-plate airfoils (Crighton 1985; Howe 1998*b*), and yields

$$\alpha(k,\omega,\eta_o) = \frac{2\sqrt{k+\mathrm{i}0}}{\sqrt{\nu+\mathrm{i}0}}\,\mathrm{e}^{-|k|\eta_o}.$$

Using this formula and summing over all frequencies ω and wavenumbers k of B_I, the value of $B = B(\xi,0,t) \equiv B(s,t)$ on the free streamline is found to be given by

$$\begin{aligned} B(\xi,0,t) &= -\frac{1}{2\pi}\int_{-\infty}^{\infty}\frac{\mathscr{F}(k,\omega)\sqrt{k+\mathrm{i}0}}{\sqrt{\nu+\mathrm{i}0}}\mathrm{e}^{\mathrm{i}(\nu\xi-\omega t)-|k|\eta_o}\,\mathrm{d}k\,\mathrm{d}\omega \\ &= -\frac{U\Gamma h\mathrm{e}^{\mathrm{i}\pi/4}}{2\pi^{3/2}(\pi+4)}\int_{-\infty}^{\infty}\left|\frac{\mathrm{d}\zeta_o}{\mathrm{d}z}(\tau)\right|^2 \mathrm{Re}\left[\frac{1}{\zeta_o^{3/2}(\tau)}\right]\frac{\mathrm{e}^{\mathrm{i}(\nu\xi-\omega(t-\tau))}\mathrm{d}\omega\,\mathrm{d}\tau}{\sqrt{\nu+\mathrm{i}0}} \qquad (3.11) \\ &= -\frac{U^{3/2}\Gamma}{2\pi h^{3/2}}\left(\frac{\pi+4}{2}\right)^{3/2}\int_{-\infty}^{t-s/U}\left|\frac{\sqrt{\zeta_o(\hat\tau)+1}}{\sqrt{\zeta_o(\hat\tau)}+\mathrm{i}}\right|^2 \\ &\quad\times\mathrm{Re}\left[\frac{1}{\zeta_o^{3/2}(\hat\tau)}\right]\frac{\mathrm{d}\tau}{\sqrt{t-s/U-\tau}} \qquad (3.12) \end{aligned}$$

where use has been made of (3.9) and (3.1*b*). Both of the alternative representations (3.11), (3.12) are used below.

3.4. *Bound vorticity on the free streamline*

The unsteady flow may be regarded as 'slipping' over the undisturbed free streamline on which the limiting value of the irrotational velocity determines the change in the slip velocity, i.e. the bound vorticity. On the free streamline $B(s,t) = -\partial\varphi/\partial t \equiv U\partial\varphi/\partial s$, where $\gamma = -\partial\varphi/\partial s$ is the unsteady component of the circulation per unit length of the free streamline (taken in the positive sense with respect to the $\boldsymbol{k}$-direction, out of the plane of the paper in figures 1(*a*) and 3) which convects as a frozen pattern on S at the free streamline velocity U (i.e. $\gamma = \gamma(t-s/U)$). In this sense the contribution to the radiation from the second integral of (2.3) is similar to that from Γ, except that the vorticity is a distribution 'bound' to the free streamline.

The total bound vorticity Γ_{S} shed from the fence at time t is

$$\Gamma_{\mathrm{S}} = -\int_{\mathrm{S}}\frac{\partial\varphi}{\partial s}(s,t)\,\mathrm{d}s, \qquad (3.13)$$

https://doi.org/10.1017/S0022112005006488 Published online by Cambridge University Press

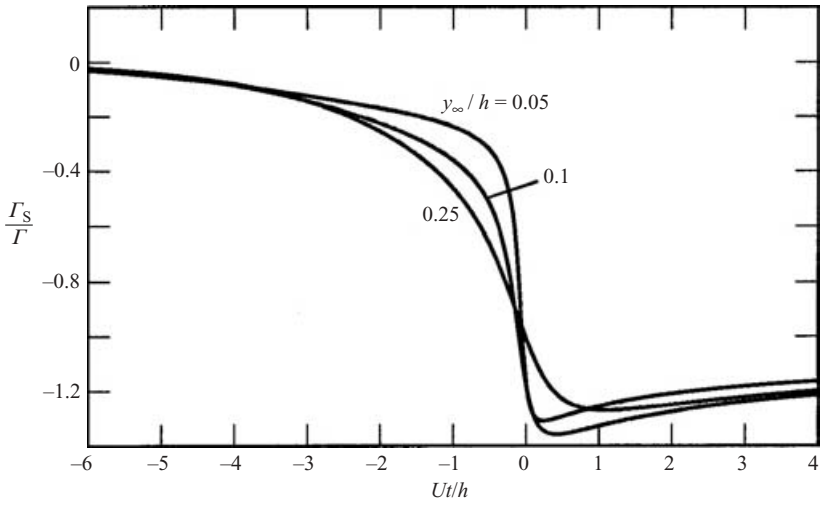


FIGURE 4. Growth of the relative bound vorticity Γ_S/Γ on the free streamline for the three cases $y_\infty/h = 0.05,\ 0.1,\ 0.25$.

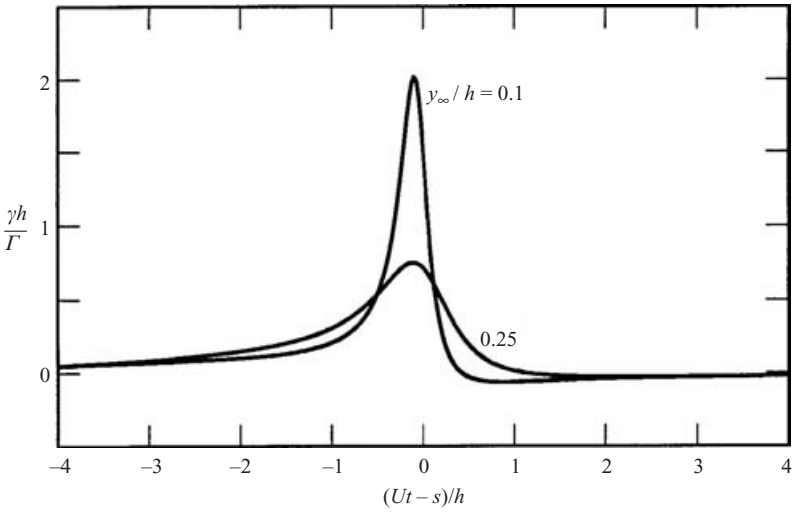


FIGURE 5. Distribution of circulation density $\gamma(t - s/U)$ on the free streamline for $y_\infty/h = 0.1,\ 0.25$.

which (3.12) permits to be expressed in the following non-dimensional form:

$$\frac{\Gamma_S(\hat{t})}{\Gamma} = \frac{1}{\pi}\left(\frac{\pi+4}{2}\right)^{3/2} \int_{-\infty}^{\hat{t}} \left|\frac{\sqrt{\zeta_o(\hat{\tau})+1}}{\sqrt{\zeta_o(\hat{\tau})}+\mathrm{i}}\right|^2 \mathrm{Re}\left[\frac{1}{\zeta_o^{3/2}(\hat{\tau})}\right] \sqrt{\hat{t}-\hat{\tau}}\,\mathrm{d}\hat{\tau}, \quad \hat{t} = \frac{Ut}{h}. \tag{3.14}$$

The growth of the overall relative bound vorticity Γ_S/Γ is plotted in figure 4 as a function of Ut/h for $y_\infty/h = 0.05,\ 0.1,\ 0.25$, the time being measured in each case from the instant of closest approach of the vortex to the tip of the fence. The total shed circulation becomes equal and opposite to that of the incident vortex when the latter attains its minimum distance from the fence, and reaches a negative maximum shortly afterwards. The circulation density $\gamma(t - s/U)$ must therefore be confined to a relatively short interval in s propagating at speed U along the free streamline. This is illustrated in figure 5, where $\gamma(t - s/U)h/\Gamma$ is plotted as a function of $(Ut - s)/h$ for

https://doi.org/10.1017/S0022112005006488 Published online by Cambridge University Press

$y_\infty/h = 0.1$ and 0.25. The points labelled on the free streamline of figure 3 represent successive locations of the peak circulation density when $y_\infty = 0.25h$. If, in a first approximation, we regard this peak as the moving centroid of a localized vortex on the free streamline, it is seen that it keeps pace with the incident vortex, and since figure 4 shows that its net circulation is essentially equal and opposite to Γ, the combined back reactions of two vortices on the unsteady motion in the neighbourhood of the fence must therefore decrease extremely fast as they pass downstream. Thus, the production of sound by the interaction of Γ with the fence can only be effective during the very short time interval in which the vortex is accelerating past the tip of the fence.

4. The acoustic radiation

4.1. *Green's function*

The hydrodynamic problem of § 3 determines the unsteady pressure distribution in the acoustic near field of the fence. At the very low mean flow Mach numbers $M = U/c_o$ that are relevant in water the wavelength of the sound generated as the vortex passes the fence is typically of order $h/M \gg h$, so that the acoustic response of the fluid becomes evident only at large distances from the fence, where $|\boldsymbol{x}| \gg h$. Lighthill's acoustic analogy equation (2.1) and its formal solution (2.3) provide the means for determining the far-field sound in terms of the calculated near field. This simplifies the evaluation of the integrals in (2.3), because an explicit functional representation of the Green's function $G(\boldsymbol{x}, \boldsymbol{y}, t-\tau)$ is required only for $|\boldsymbol{x}| \gg h$, and only in the acoustically compact limit in which the characteristic wavelength of the sound is also much larger than h.

Symmetry arguments (confirmed by routine analysis: Howe 1998*a*; Young *et al.* 2005) show that the compact approximation $G_0(\boldsymbol{x}, \boldsymbol{y}, t-\tau)$, say, to Green's function for the geometrically much simpler problem of figure 1(*b*), where there is no fence and the free streamline and cavity begin at O, is equal to just twice the corresponding Green's function for a thin, rigid half-plane in the absence of separation and the cavity (so that sound can also propagate freely to infinity in the lower region $x_2 < 0$ of figure 1*b*). The compact approximation for the half-plane was determined by Howe (1975, 1998*b*) and using it we find for the cavity flow problem of figure 1(*b*)

$$G_0(\boldsymbol{x}, \boldsymbol{y}, t-\tau) = \frac{2\phi(\boldsymbol{y})\sin\left(\frac{1}{2}\theta\right)}{\pi\sqrt{r}}\,\delta\left(t-\tau-\frac{|\boldsymbol{x}|}{c_o}\right), \quad |\boldsymbol{x}| \to \infty, \tag{4.1}$$

where $\boldsymbol{x} = (x_1, x_2) = r(\cos\theta, \sin\theta)$ and

$$\phi(\boldsymbol{y}) = \mathrm{Re}\,(-\mathrm{i}\sqrt{z}), \quad z = y_1 + \mathrm{i}y_2. \tag{4.2}$$

This result can be generalized to determine the corresponding Green's function $G(\boldsymbol{x}, \boldsymbol{y}, t-\tau)$ for the geometry of figure 1(*a*). To do this, note first that the functional form of $\phi(\boldsymbol{y})$ ensures that G_0 satisfies the conditions of figure 1(*b*), namely that $\partial G_0/\partial y_n = 0$, $G_0 = 0$ respectively on $y_1 \lesseqgtr 0$, $y_2 = 0$. Also, at large acoustic wavelengths and for observer and source positions at large distances from the fence ($|\boldsymbol{x}|$, $|\boldsymbol{y}| \gg h$), the geometry of the fence and wall of figure 1(*a*) will be indistinguishable from the plane wall analogue of figure 1(*b*). Thus, viewed on this scale the compact Green's function for figure 1(*a*) must coincide with (4.1). The actual Green's function for the fence and source positions $\boldsymbol{y} \sim O(h)$ is therefore obtained merely by replacing the

https://doi.org/10.1017/S0022112005006488 Published online by Cambridge University Press

function $\phi(\boldsymbol{y})$ (which is applicable when $|\boldsymbol{y}| \gg h$) by

$$\Phi(\boldsymbol{y}) = \mathrm{Re}\left(-\mathrm{i}\sqrt{\frac{2h\zeta(z)}{\pi+4}} \right), \quad z = y_1 + \mathrm{i}y_2. \tag{4.3}$$

Hence

$$G(\boldsymbol{x}, \boldsymbol{y}, t-\tau) = \frac{2\Phi(\boldsymbol{y}) \sin\left(\frac{1}{2}\theta\right)}{\pi\sqrt{r}}\, \delta\left(t - \tau - \frac{|\boldsymbol{x}|}{c_o}\right), \quad r \equiv |\boldsymbol{x}| \to \infty, \tag{4.4}$$

which evidently satisfies $G = 0$ on the free streamline and $\partial G/\partial y_n = 0$ on the wetted sections of the wall and fence, and has the correct behaviour for $|\boldsymbol{y}| \gg h$ where $\Phi(\boldsymbol{y}) \sim \phi(\boldsymbol{y})$.

According to (4.4) the sound spreads out cylindrically from the source region (as appropriate for two-dimensional source distributions), decaying as $1/\sqrt{r}$ at large distances with the directionality $\sin(\theta/2)$, which vanishes in downstream directions close to the pressure-release free streamline, and peaks in the direction directly upstream of the fence.

4.2. *Direct radiation from the vortex*

At infinitesimal Mach number and at large distances from the fence, the acoustic component of $B(\boldsymbol{x}, t) \approx p(\boldsymbol{x}, t)/\rho_o$, where $p(\boldsymbol{x}, t)$ is the acoustic pressure perturbation. The first integral in (2.3) is the contribution p_Γ, say, to this pressure produced by the direct interaction of the vortex with the fence, when the influence of vortex shedding is ignored.

Evaluating the integral using (4.4) we find

$$\frac{p_\Gamma(\boldsymbol{x}, t)}{\left(\frac{\rho_o U \Gamma}{h}\right)\left(\frac{h}{r}\right)^{1/2} \sin\left(\frac{1}{2}\theta\right)} \approx -\frac{2\sqrt{h}}{\pi U}\left[v_o \frac{\partial \Phi}{\partial y_n} \right]$$

$$= -\frac{1}{\pi}\left(\frac{\pi+4}{2}\right)^{1/2}\left[\left| \frac{\sqrt{\zeta_o+1}}{\sqrt{\zeta_o}+\mathrm{i}} \right|^2 \mathrm{Re}\left(\frac{1}{\sqrt{\zeta_o}}\right) \right], \quad r = |\boldsymbol{x}| \to \infty, \tag{4.5}$$

where the square brackets indicate evaluation at the retarded time $[t] = t - |\boldsymbol{x}|/c_o$, i.e. at the retarded position $\boldsymbol{y} = \boldsymbol{x}_o([t])$ of the vortex in the physical plane, and in the ζ-plane at $\zeta_o = \xi_o([\hat{t}]) + \mathrm{i}\eta_o$ ($\hat{t} = Ut/h$).

The curves labelled p_Γ in figures 6 and 7 illustrate the non-dimensional waveform determined by (4.5) respectively for $y_\infty/h = 0.25$ and 0.1. The trajectories of the vortex and the centroid of the free-streamline circulation density $\gamma(t - s/U)$ are also plotted in upper part of figure 7 (see figure 3 for the corresponding plots for $y_\infty/h = 0.25$). In both cases p_Γ has the form of a sharp-fronted, negative pulse whose front develops rapidly at the retarded time at which the vortex passes close to the tip of the fence; the pulse decays slowly at later times and is still significant when the retarded position of the vortex is several fence heights downstream.

4.3. *The overall acoustic radiation*

The second integral of (2.3) determines the component $p_S(\boldsymbol{x}, t)$ of the acoustic pressure attributable to the bound vorticity on the free streamline. It is readily evaluated using

https://doi.org/10.1017/S0022112005006488 Published online by Cambridge University Press

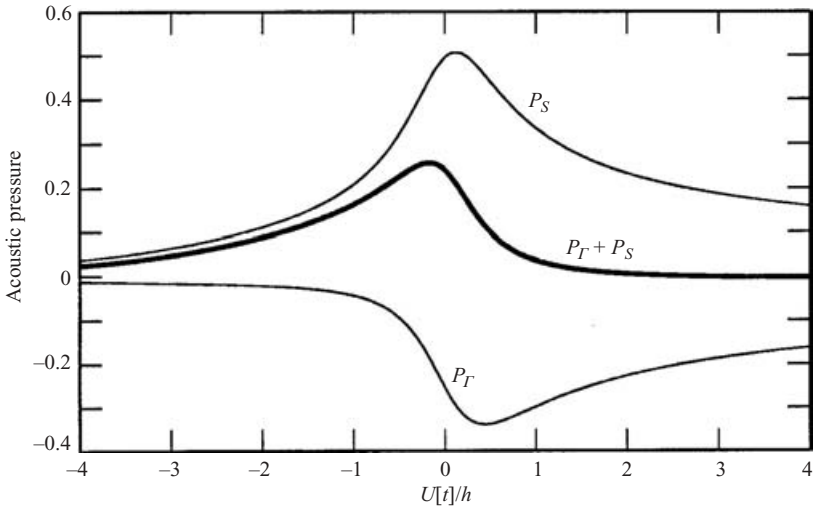


FIGURE 6. The non-dimensional, far-field acoustic pressures (p_Γ, p_S and $p_\Gamma + p_S$)/$(\rho_o U\Gamma/h)(h/r)^{1/2}\sin(\frac{1}{2}\theta)$ plotted as functions of the retarded time $t - |\boldsymbol{x}|/c_o$ for $y_\infty/h = 0.25$.

(4.4) and the representation (3.11) of $B(s,\tau)$ on S. The definition (4.3) implies that

$$\frac{\partial G}{\partial y_n} = \frac{1}{\pi\sqrt{\xi}}\left(\frac{\pi+4}{2h}\right)^{1/2}\frac{\sin\left(\frac{1}{2}\theta\right)}{\sqrt{r}}\delta\left(t-\tau-\frac{|\boldsymbol{x}|}{c_o}\right) \quad \text{on S, where } \xi > 0,\ \eta = 0.$$

The integration with respect to s is performed explicitly by recalling that $\mathrm{d}s = 2h\,\mathrm{d}\xi/(\pi+4)$ on S, leading to

$$\frac{p_S(\boldsymbol{x},t)}{\left(\frac{\rho_o U\Gamma}{h}\right)\left(\frac{h}{r}\right)^{1/2}\sin\left(\frac{1}{2}\theta\right)} \approx -\frac{Uh}{2\pi}\left(\frac{2}{\pi+4}\right)^{1/2}\int_{-\infty}^{[t]}\left|\frac{\mathrm{d}\zeta_o}{\mathrm{d}z}(\tau)\right|^2 \mathrm{Re}\left(\frac{1}{\zeta_o^{3/2}(\tau)}\right)\mathrm{d}\tau,$$

$$r = |\boldsymbol{x}| \to \infty. \qquad (4.6)$$

The integrand is evaluated along the path of the incident vortex determined by the solution of equation (3.3). But that equation implies that

$$\left|\frac{\mathrm{d}\zeta_o}{\mathrm{d}z}(\tau)\right|^2 = \left(\frac{\pi+4}{2hU}\right)\frac{\partial\zeta_o}{\partial\tau}, \qquad (4.7)$$

and this permits (4.6) to be evaluated explicitly in the form

$$\frac{p_S(\boldsymbol{x},t)}{\left(\frac{\rho_o U\Gamma}{h}\right)\left(\frac{h}{r}\right)^{1/2}\sin\left(\frac{1}{2}\theta\right)} \approx \frac{1}{\pi}\left(\frac{\pi+4}{2}\right)^{1/2}\mathrm{Re}\left[\frac{1}{\sqrt{\zeta_o}}\right], \quad r = |\boldsymbol{x}| \to \infty, \qquad (4.8)$$

where the square brackets indicate evaluation at $[t] = t - |\boldsymbol{x}|/c_o$.

The corresponding acoustic pressure profiles for $y_\infty/h = 0.25,\ 0.1$ are plotted in figures 6 and 7, together with the overall acoustic pressure $p = p_\Gamma + p_S$, given (in the

https://doi.org/10.1017/S0022112005006488 Published online by Cambridge University Press

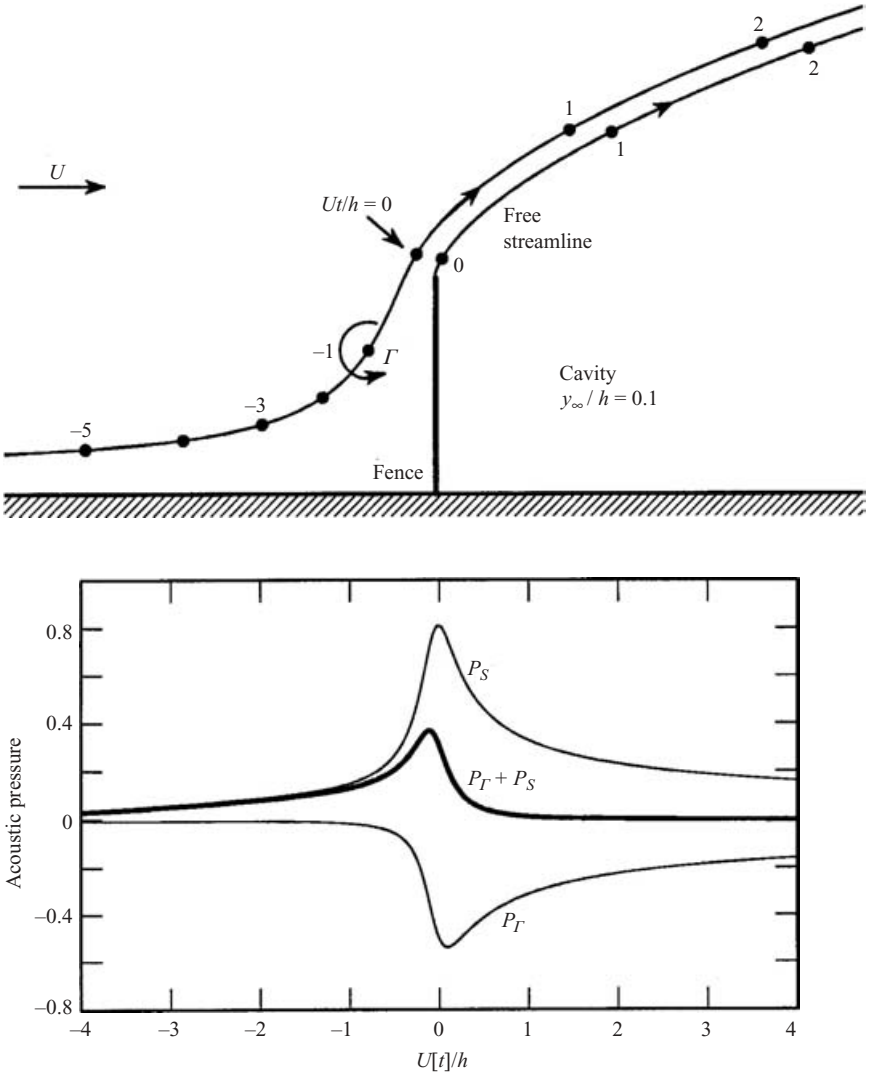


FIGURE 7. The non-dimensional, far-field acoustic pressures (p_Γ, p_S and $p_\Gamma + p_S$)/$(\rho_o U\Gamma/h)(h/r)^{1/2}\sin\left(\frac{1}{2}\theta\right)$ plotted as functions of the retarded time $t - |\boldsymbol{x}|/c_o$ for $y_\infty/h = 0.1$. The corresponding trajectories of Γ and the peak of the free-streamline circulation density $\gamma(t - s/U)$ are shown in the upper part of the figure.

same notation) by

$$\frac{p(\boldsymbol{x},t)}{\left(\dfrac{\rho_o U\Gamma}{h}\right)\left(\dfrac{h}{r}\right)^{1/2}\sin\left(\frac{1}{2}\theta\right)} \approx -\frac{1}{\pi}\left(\frac{\pi+4}{2}\right)^{1/2}\mathrm{Re}\left[\frac{1}{\sqrt{\zeta_o}}\left(\left|\frac{\sqrt{\zeta_o}+1}{\sqrt{\zeta_o}+\mathrm{i}}\right|^2 - 1\right)\right]. \quad (4.9)$$

Evidently the profile of p_S is similar in shape but opposite in sign to the directly radiated pressure p_Γ, being a sharply fronted pulse followed by a slowly decaying tail. The tails are effectively equal and opposite and therefore ultimately produce equal

https://doi.org/10.1017/S0022112005006488 Published online by Cambridge University Press

and opposite contributions to the sound, because

$$\left|\frac{\sqrt{\zeta_o+1}}{\sqrt{\zeta_o}+\mathrm{i}}\right|^2 \to 1$$

at large retarded times, when Γ and the centroid of the bound vorticity proceed downstream as a 'vortex pair' of approximately zero net circulation, on parallel streamlines (on which $\partial\Phi/\partial y_n$ assumes approximately equal values) and at essentially the same convection velocity $\sim U$. The two components differ in strength only at those retarded times when Γ is close to the tip of the fence, so that the overall acoustic waveform consists of a short positive pulse whose width progressively decreases as $y_\infty/h \to 0$.

In the formal limit in which $y_\infty/h \sim +0$ the vortex follows a trajectory immediately adjacent to the wetted surfaces of the wall and fence and subsequently convects along the free streamline. Then

$$\zeta_o(\tau) = \left(\frac{\pi+4}{2}\right)\frac{U\tau}{h} + \mathrm{i}0$$

and the overall pressure given by (4.9) vanishes identically for all values of the retarded times $[t]$. This predicted cancellation of the net radiation is a consequence of the linearized approximation, according to which both Γ and the shed vorticity convect at the same mean flow velocity. In the analogous flow of figure 1(*b*), involving a cavity bounded by a free streamline continuation of the wall, linear theory requires that Γ and the shed vorticity convect at the same velocity U, and the acoustic pressures produced by each are always equal and opposite (Howe 1976, 1998*b*).

5. Conclusion

Aeroacoustic sources close to the sharp edge of an acoustically non-compact body are known to generate sound with great efficiency. In free space the amplitude of the acoustic pressure radiated by a low-Mach-number ($M \ll 1$), three-dimensional localized source (i.e. by a 'quadrupole') is proportional to $\rho_o v^2 M^2$, v being a typical velocity in the source flow. The amplitude of sound generated by the same source near the trailing edge of a large airfoil is larger by a factor $\sim 1/M^{3/2}$. When the source and edge region can be regarded as two-dimensional over distances comparable to the acoustic wavelength (as in figure 1*b*) the efficiency is increased further and the amplitude becomes $O(\rho_o v^2)$, and independent of the aeroacoustic 'source type' (dipole, quadrupole, etc.). This latter conclusion has been shown in § 4 to apply when the region downstream of the trailing edge is a nominally steady vacuous cavity formed by water flowing over a 'fence' on a flat wall.

The equations describing aeroacoustic edge-interaction problems of this type can always be linearized in a first approximation. The assumption is made that turbulence quadrupole sources in the impinging flow are swept past the edge by the locally steady mean flow, with no account taken of nonlinear back reaction on the source motion produced by 'images' in the solid boundaries. The canonical problem treated in this paper has taken the impinging disturbance to be a line vortex Γ. The vortex induces the shedding of additional vorticity from the tip of the fence in order to maintain a smooth flow at the edge (the Kutta condition). According to linear theory, the shed vorticity convects at the constant uniform mean flow speed U within a sheet of 'bound' vorticity on the undisturbed free streamline. A strong peak in the bound vorticity is established when Γ is near its point of closest approach to the tip of the fence; it forms a concentrated zone of vorticity on the free streamline with overall

https://doi.org/10.1017/S0022112005006488 Published online by Cambridge University Press

circulation $\sim -\Gamma$ and subsequently 'keeps pace' with the incident vortex Γ as the latter travels downstream along a parallel trajectory adjacent to the cavity. Both the incident and the shed vorticity generate sound by interaction with the fence, but their respective contributions to the acoustic pressure are of opposite phase and tend to cancel, so that the overall level of the radiation depends on a delicate balance between the opposing sources. The dominant radiation in the form of a pressure pulse of width $\sim h/M$ is produced when the vortex passes the fence tip; at later times the two opposing sources become effectively equal and opposite – the 'dipole', to which the isolated vortex is equivalent, is transformed into a weaker quadrupole by an equal and opposite image vortex in the free streamline. In the simpler problem of figure 1(*b*), where the cavity is formed immediately downstream of the edge of a half-plane, the two opposing sources are equal and opposite for all times and linear theory predicts that the flow is silent.

These conclusions are based on the hypothesis that the vacuous wake extends downstream a distance at least of the order of the acoustic wavelength, so that the sound waves are launched above a non-compact pressure-release surface.

REFERENCES

Batchelor, G. K. 1967 *An Introduction to Fluid Dynamics*. Cambridge University Press.

Birkhoff, G. & Zarantonello, E. H. 1957 *Jets, Wakes and Cavities*. Academic.

Blake, W. K. 1986 *Mechanics of Flow-induced Sound and Vibration*, Volume 2: *Complex Flow-Structure Interactions*. Academic.

Chandiramani, K. L. 1974 Diffraction of evanescent waves, with applications to aerodynamically scattered sound and radiation from unbaffled plates. *J. Acoust. Soc. Am.* **55**, 19–29.

Chase, D. M. 1972 Sound radiated by turbulent flow off a rigid hal-plane as obtained from a wavevector spectrum of hydrodynamic pressure. *J. Acoust. Soc. Am.* **52**, 1011–1023.

Chase, D. M. 1975 Noise radiated from an edge in turbulent flow. *AIAA J.* **13**, 1041–1047.

Crighton, D. G. 1975 Basic principles of aerodynamic noise generation. *Prog. Aerospace Sci.* **16**, 31–96.

Crighton, D. G. 1985 The Kutta condition in unsteady flow. *Annu. Rev. Fluid Mech.* **17**, 411–445.

Ffowcs Williams, J. E. 1974 Sound production at the edge of a steady flow. *J. Fluid Mech.* **66**, 791–816.

Ffowcs Williams, J. E. & Hall, L. H. 1970 Aerodynamic sound generation by turbulent flow in the vicinity of a scattering half-plane. *J. Fluid Mech.* **40**, 657–670.

Gurevich, M. I. 1965 *Theory of Jets in Ideal Fluids*. Academic.

Howe, M. S. 1975 Contributions to the theory of aerodynamic sound, with application to excess jet noise and the theory of the flute. *J. Fluid Mech.* **71**, 625–673.

Howe, M. S. 1976 The influence of vortex shedding on the generation of sound by convected turbulence. *J. Fluid Mech.* **76**, 711–740.

Howe, M. S. 1998*a* Surface pressure and sound produced by turbulent pressure-release edge flow. *Pennsylvania State University, Applied Research Laboratory Tech. Mem.* 98–148.

Howe, M. S. 1998*b* *Acoustics of Fluid-Structure Interactions*, Cambridge University Press.

Lamb, H. 1932 *Hydrodynamics*, 6th. edn. Cambridge University Press.

Noble, B. 1958 *Methods based on the Wiener-Hopf Technique*. Pergamon.

Rayleigh, Lord 1876 On the resistance of fluids. *Phil. Mag.* II, 430–441 (also *Scientific Papers*, Volume I, pp. 287–296.)

Young, S. D., Brungart, T. A. & Lauchle, G. C. 2004 Effect of a downstream ventilated gas cavity on the spectrum of turbulent boundary layer wall pressure fluctuations. *Proc. IMECE 04, 2004 ASME International Mechanical Engineering Congress, November 13–19, Anaheim, California.*

Young, S. D., Brungart, T. A., Lauchle, G. C. & Howe, M. S. 2005 Effect of a downstream ventilated gas cavity on the spectrum of turbulent boundary layer wall pressure fluctuations. *J. Acoust. Soc. Am.* (in press).

https://doi.org/10.1017/S0022112005006488 Published online by Cambridge University Press